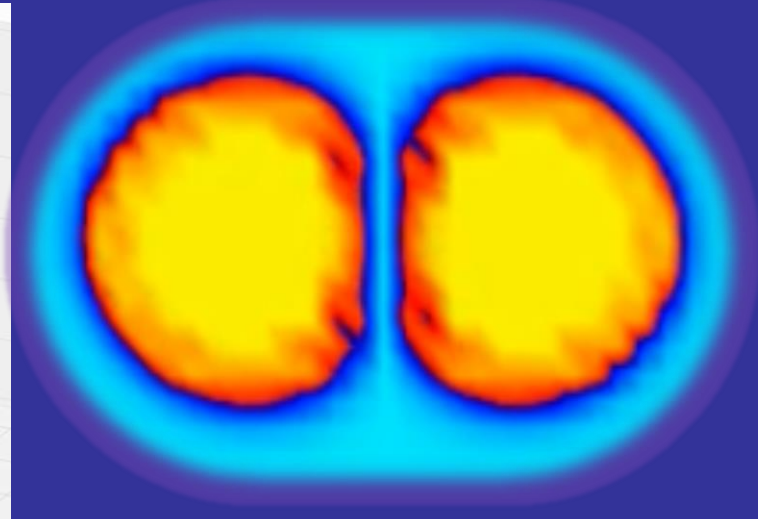
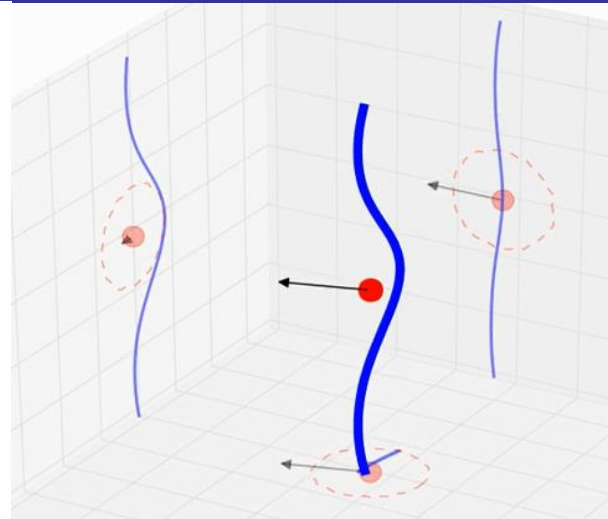
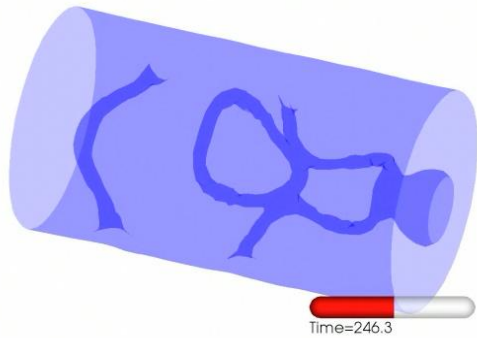


Selected aspects of superfluid dynamics in nuclear systems



Piotr Magierski (Warsaw University of Technology)

Collaborators: Aurel Bulgac (Univ. of Washington)
Kenneth J. Roche (PNNL)
Kazuyuki Sekizawa (Warsaw Univ. of Technology)
Ionel Stetcu (LANL)
Gabriel Wlazłowski (Warsaw Univ. of Technology)

Outline

- Relativistic Coulomb excitation.
- Pairing dynamics in nuclear collisions.
- Effective mass of nuclear impurity in superfluid neutron matter.

GOAL:

Description of superfluid dynamics far from equilibrium within the framework of Time Dependent Density Functional Theory (TDDFT) (- see Aurel's and Gabriel's talks)

We would like to describe the time evolution of (externally perturbed) spatially inhomogeneous, superfluid Fermi system and in particular such phenomena as:

- Vortex dynamics in ultracold Fermi gases and neutron matter (see Gabriel's talk).
- Quantum turbulence (see Gabriel's talk).
- Atomic cloud collisions.
- Nuclear dynamics:
induced nuclear fission, reactions, fusion, excitation of nuclei with gamma rays and neutrons (see also Aurel's talk).

Formalism for Time Dependent Phenomena: TDSLDA

Local density approximation (no memory terms)

$$i\hbar \frac{\partial}{\partial t} \begin{pmatrix} u_{k\uparrow}(\mathbf{r}, t) \\ u_{k\downarrow}(\mathbf{r}, t) \\ v_{k\uparrow}(\mathbf{r}, t) \\ v_{k\downarrow}(\mathbf{r}, t) \end{pmatrix} = \begin{pmatrix} h_{\uparrow,\uparrow}(\mathbf{r}, t) & h_{\uparrow,\downarrow}(\mathbf{r}, t) & 0 & \Delta(\mathbf{r}, t) \\ h_{\downarrow,\uparrow}(\mathbf{r}, t) & h_{\downarrow,\downarrow}(\mathbf{r}, t) & -\Delta(\mathbf{r}, t) & 0 \\ 0 & -\Delta^*(\mathbf{r}, t) & -h_{\uparrow,\uparrow}^*(\mathbf{r}, t) & -h_{\uparrow,\downarrow}^*(\mathbf{r}, t) \\ \Delta^*(\mathbf{r}, t) & 0 & -h_{\uparrow,\downarrow}^*(\mathbf{r}, t) & -h_{\downarrow,\downarrow}^*(\mathbf{r}, t) \end{pmatrix} \begin{pmatrix} u_{k\uparrow}(\mathbf{r}, t) \\ u_{k\downarrow}(\mathbf{r}, t) \\ v_{k\uparrow}(\mathbf{r}, t) \\ v_{k\downarrow}(\mathbf{r}, t) \end{pmatrix}$$

Density functional contains normal densities, anomalous density (pairing) and currents:

$$E(t) = \int d^3r \left[\varepsilon(n(\vec{r}, t), \tau(\vec{r}, t), \nu(\vec{r}, t), \vec{j}(\vec{r}, t)) + V_{ext}(\vec{r}, t)n(\vec{r}, t) + \dots \right]$$

- The system is placed on a large 3D spatial lattice.
- No symmetry restrictions
- Number of PDEs is of the order of the number of spatial lattice points

Current capabilities of the code:

- volumes of the order of ($L = 80^3$) capable of simulating time evolution of 42000 neutrons at saturation density (natural application: neutron stars)
- capable of simulating up to times of the order of 10^{-19} s (a few million time steps)
- CPU vs GPU on Titan ≈ 15 speed-up (likely an additional factor of 4 possible)

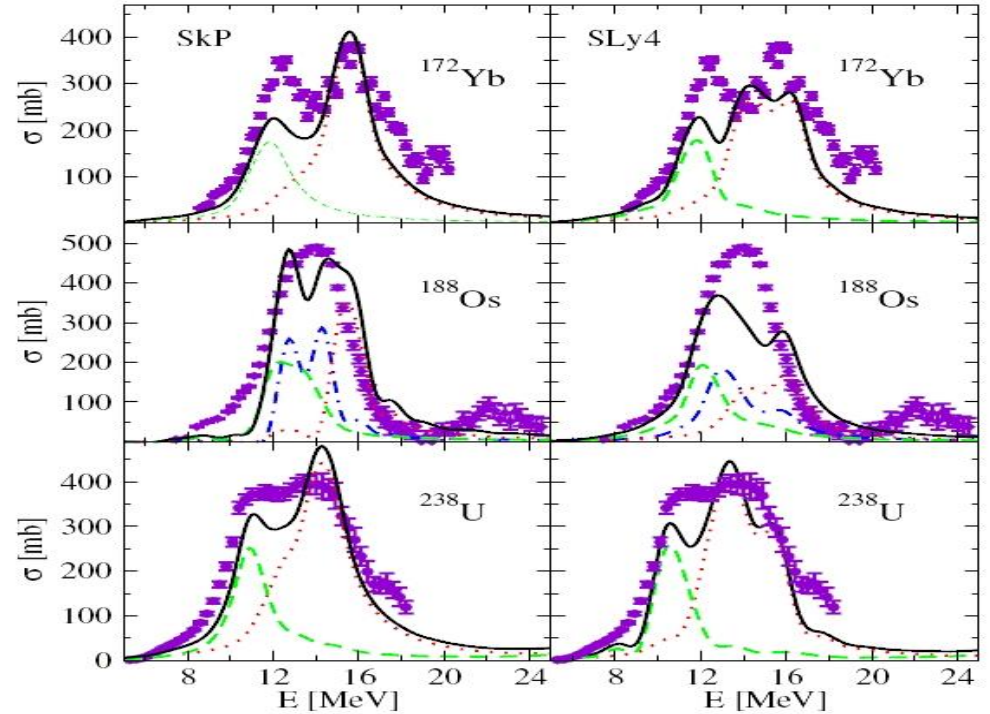
Eg. for 137062 two component wave functions:

CPU version (4096 nodes x 16 PEs) - 27.90 sec. for 10 time steps

GPU version (4096 PEs + 4096GPU) - 1.84 sec. for 10 time step

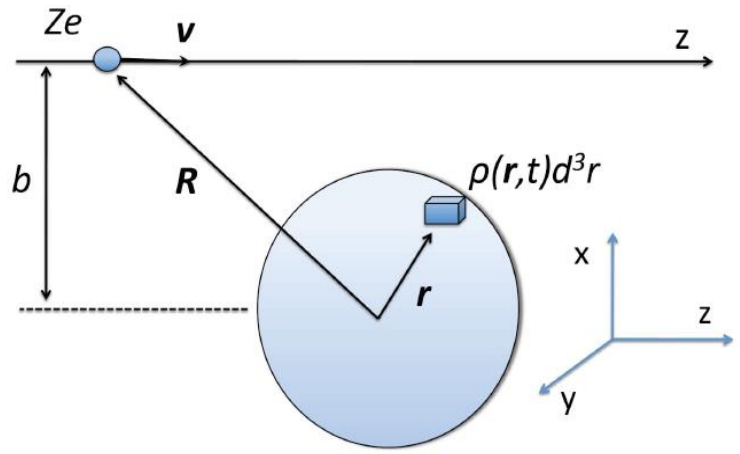
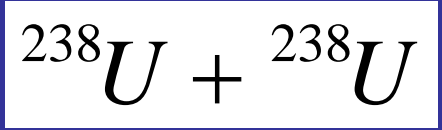
**Linear response regime:
GDR of deformed nuclei**

Photoabsorption cross section →



I. Stetcu, A. Bulgac, P. Magierski, K.J. Roche,
Phys. Rev. C84 051309 (2011)

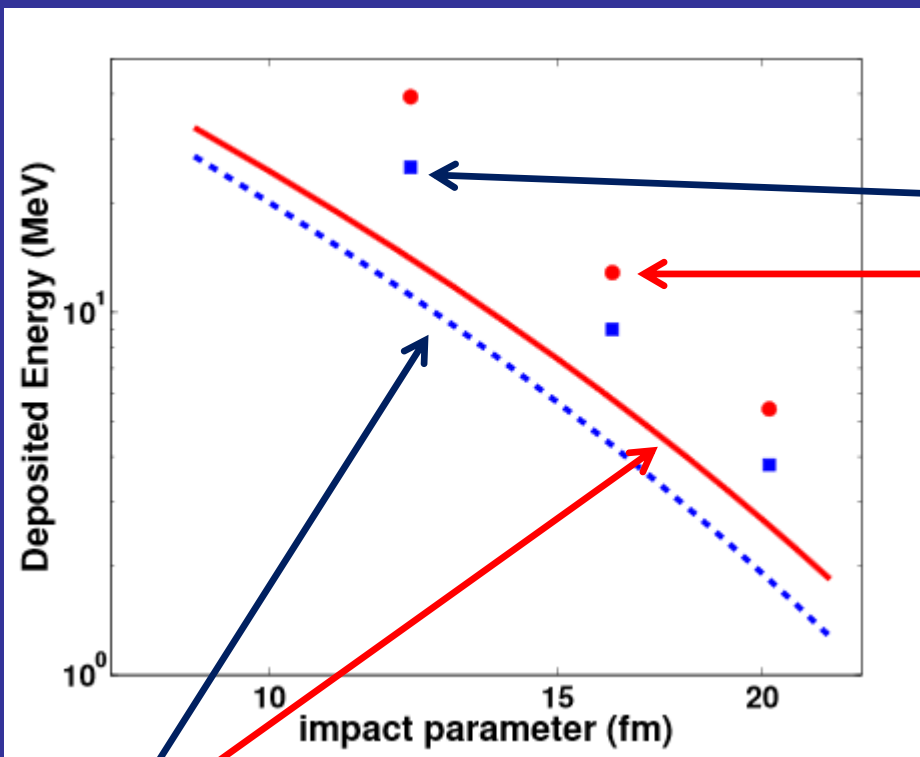
**Beyond linear regime:
Relativistic Coulomb excitation:**



$$\hbar\omega \approx \frac{\hbar}{\tau_{coll}} = \frac{\gamma v}{b} \approx 12\text{MeV} \quad ; \quad \gamma = \frac{1}{\sqrt{1 - (v/c)^2}}$$

I. Stetcu, C. Bertulani, A. Bulgac, P. Magierski, K.J. Roche
Phys. Rev. Lett. 114, 012701 (2015)

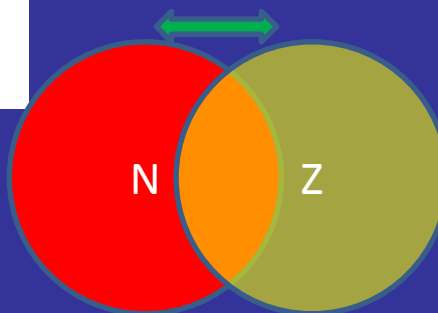
Energy transferred to the target nucleus in the form of internal excitations



TDSLDA – parallel orientation

TDSLDA – perpendicular orientation

Goldhaber-Teller like model:
proton and neutron density distributions
oscillating against each other



Two characteristic frequencies:

$$\hbar\omega_1 = 12\text{MeV}$$

$$\hbar\omega_2 = 16\text{MeV}$$

Part of the energy is transferred
to other degrees of freedom
than pure dipole moment oscillations.

Coupling to e.m. field:

$$\vec{E} = -\vec{\nabla}\phi - \frac{1}{c} \frac{\partial \vec{A}}{\partial t}$$

$$\vec{B} = \vec{\nabla} \times \vec{A}$$

$$\vec{\nabla}\psi \rightarrow \vec{\nabla}_A\psi = \left(\vec{\nabla} - i\frac{e}{\hbar c} \vec{A} \right) \psi$$

$$\vec{\nabla}\psi^* \rightarrow \vec{\nabla}_{-A}\psi^* = \left(\vec{\nabla} + i\frac{e}{\hbar c} \vec{A} \right) \psi^*$$

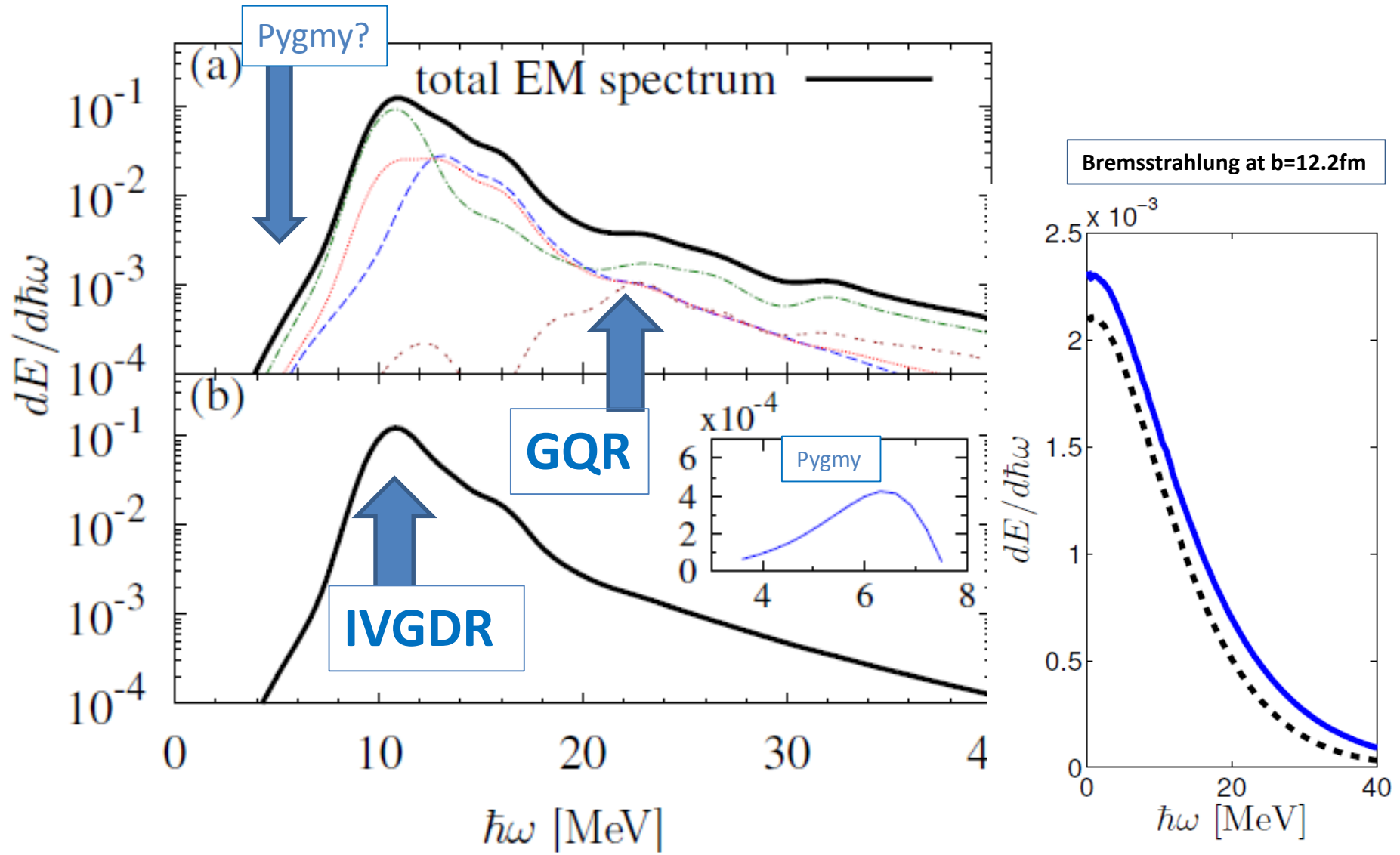
$$i\hbar \frac{\partial}{\partial t} \psi \rightarrow \left(i\hbar \frac{\partial}{\partial t} - e\phi \right) \psi$$

which implies that $\vec{\nabla}\psi\psi^* \rightarrow \vec{\nabla}\psi\psi^*$.

Consequently the densities change according to:

- density: $\rho_A(\mathbf{r}) = \rho_A(\mathbf{r})$
- spin density: $\vec{s}_A(\mathbf{r}) = \vec{s}(\mathbf{r})$
- current: $\vec{j}_A(\mathbf{r}) = \vec{j}(\mathbf{r}) - \frac{e}{\hbar c} \vec{A} \rho(\mathbf{r})$
- spin current (2nd rank tensor): $\mathbf{J}_A(\mathbf{r}) = \mathbf{J}(\mathbf{r}) - \frac{e}{\hbar c} \vec{A} \otimes \vec{s}(\mathbf{r})$
- spin current (vector): $\vec{J}_A(\mathbf{r}) = \vec{J}(\mathbf{r}) - \frac{e}{\hbar c} \vec{A} \times \vec{s}(\mathbf{r})$
- kinetic energy density: $\tau_A(\mathbf{r}) = \left(\vec{\nabla} - i\frac{e}{\hbar c} \vec{A} \right) \cdot \left(\vec{\nabla}' + i\frac{e}{\hbar c} \vec{A} \right) \rho(\mathbf{r}, \mathbf{r}')|_{r=r'}$
 $= \tau(\mathbf{r}) - 2\frac{e}{\hbar c} \vec{A} \cdot \vec{j}(\mathbf{r}) + \frac{e^2}{\hbar^2 c^2} |\vec{A}|^2 \rho(\mathbf{r}) = \tau(\mathbf{r}) - 2\frac{e}{\hbar c} \vec{A} \cdot \vec{j}_A(\mathbf{r}) - \frac{e^2}{\hbar^2 c^2} |\vec{A}|^2 \rho(\mathbf{r})$
- spin kinetic energy density: $\vec{T}_A(\mathbf{r}) = \left(\vec{\nabla} - i\frac{e}{\hbar c} \vec{A} \right) \cdot \left(\vec{\nabla}' + i\frac{e}{\hbar c} \vec{A} \right) \vec{s}(\mathbf{r}, \mathbf{r}')|_{r=r'}$
 $= \vec{T}(\mathbf{r}) - 2\frac{e}{\hbar c} \vec{A}^T \cdot \mathbf{J}(\mathbf{r}) + \frac{e^2}{\hbar^2 c^2} |\vec{A}|^2 \vec{s}(\mathbf{r}) = \vec{T}(\mathbf{r}) - 2\frac{e}{\hbar c} \vec{A}^T \cdot \mathbf{J}_A(\mathbf{r}) - \frac{e^2}{\hbar^2 c^2} |\vec{A}|^2 \vec{s}(\mathbf{r})$

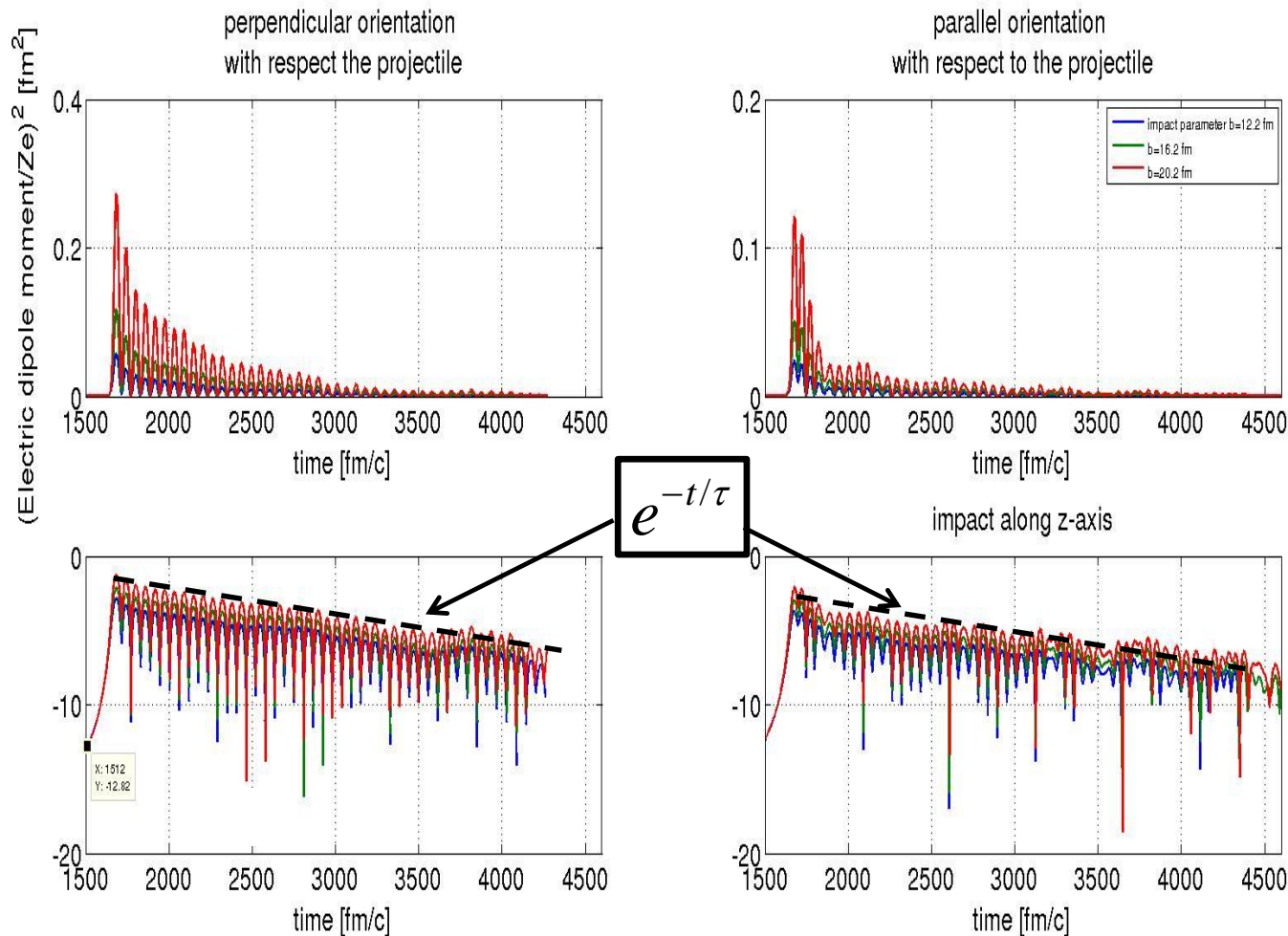
Electromagnetic radiation due to the internal nuclear motion



I. Stetcu, C. Bertulani, A. Bulgac, P. Magierski, K.J. Roche
Phys. Rev. Lett. 114, 012701 (2015)

One body dissipation can be fully accounted for in this formalism

Damping of GDR (excited ion coulex reaction) due to one-body dissipation mechanism:



$$E_{coll}(t) \propto e^{-t/\tau}; \quad \tau \approx 500 \text{ fm} / c \Rightarrow \Gamma_{\downarrow} \approx 0.4 \text{ MeV}$$

$$E_{coll}(t) \propto [D_{\max}(t)]^2$$

Physics of two nuclear, coupled superconductors

Little bit of history:

Volume 1, number 7

PHYSICS LETTERS

1 July 1962

POSSIBLE NEW EFFECTS IN SUPERCONDUCTIVE TUNNELLING *

B. D. JOSEPHSON

Cavendish Laboratory, Cambridge, England

Received 8 June 1962

We here present an approach to the calculation of tunnelling currents between two metals that is sufficiently general to deal with the case when both metals are superconducting. In that case new effects are predicted, due to the possibility that electron pairs may tunnel through the barrier leaving the quasi-particle distribution unchanged.

Dynamics of the Josephson effect:

$$J(t) = J_c \sin(\Delta\varphi(t))$$
$$\frac{d(\Delta\varphi)}{dt} = \frac{2eU}{\hbar}$$

AN ANALOG OF THE JOSEPHSON EFFECT IN NUCLEAR TRANSFORMATIONS

V. I. GOL'DANSKIĬ and A. I. LARKIN

Institute of Chemical Physics, Academy of Science, U.S.S.R.

Submitted March 30, 1967

Zh. Eksp. Teor. Fiz. 53, 1032-1037 (September, 1967)

When nuclei are bombarded by heavy ions, various processes of nucleon tunneling through the potential barrier that separates the interacting nuclei at the smallest possible classical distance are observed. It is shown that nucleon pairing may give rise to a significant increase of the cross section for the transition of neutron or proton pairs, a phenomenon which in some respects is analogous to the Josephson effect in superconductors. Pairing is taken into account in the calculation of the probability for the excitation of various levels by one-nucleon exchange, which has been calculated earlier by Breit and Ebel^[1] without such corrections. The probability for two-nucleon exchange is determined. An expression is obtained for the two-proton radioactivity with account of any number of arbitrary levels, which goes over into the Galitskii-Chel'tsov formula^[2] in the limiting case of a single S level.

Volume 32B, number 6

PHYSICS LETTERS

17 August 1970

ON A NUCLEAR JOSEPHSON EFFECT IN HEAVY ION SCATTERING

K. DIETRICH

Niels Bohr Institute, Copenhagen, Denmark*

Received 3 June 1970

The transfer of a pair of nucleons in sub-Coulomb scattering of two heavy ions is treated in a semi-classical theory. If both reaction partners are superconducting, a large enhancement factor is found.

Brief Reports

*Brief Reports are short papers which report on completed research or are addenda to papers previously published in the **Physical Review**. A Brief Report may be no longer than $3\frac{1}{2}$ printed pages and must be accompanied by an abstract.*

Weak evidence for a nuclear Josephson effect in the $^{34}\text{S}(^{32}\text{S}, ^{32}\text{S})$ elastic scattering reaction

Michel C. Mermaz

*Service de Physique Nucléaire—Métrologie Fondamentale, Centre d'Etudes Nucléaires de Saclay,
91191 Gif-sur-Yvette Cedex, France*

(Received 30 March 1987)

Optical model and exact finite range distorted-wave Born approximation analyses were performed on neutron pair exchange and alpha particle exchange reactions between two identical colliding cores. The possibility of a nuclear Josephson effect is discussed.

Neutron pair and proton pair transfer reactions between identical cores in the sulfur region

Michel C. Mermaz

Commissariat à l'Energie Atomique, Service de Physique Nucléaire, Centre d'études de Saclay, 91191 Gif sur Yvette, Cedex, France

Michel Girod

Commissariat à l'Energie Atomique, Service de Physique et Techniques Nucléaires, Boîte Postale 12, 91680 Bruyères-le-Châtel, France

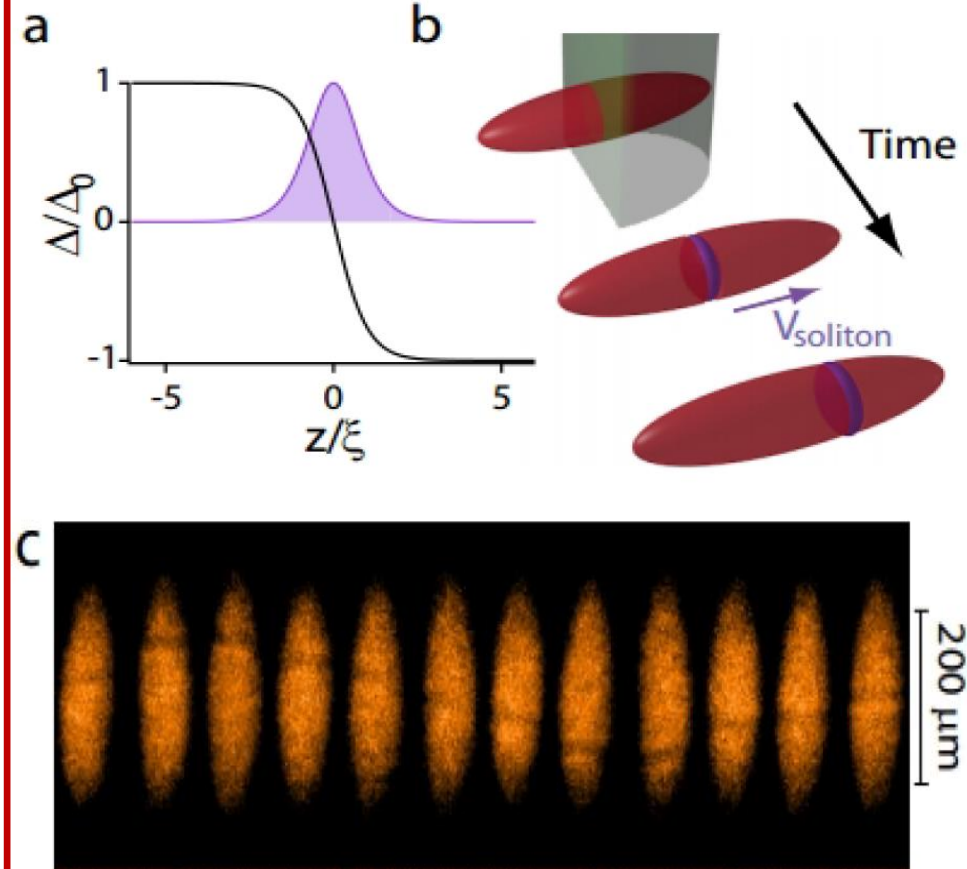
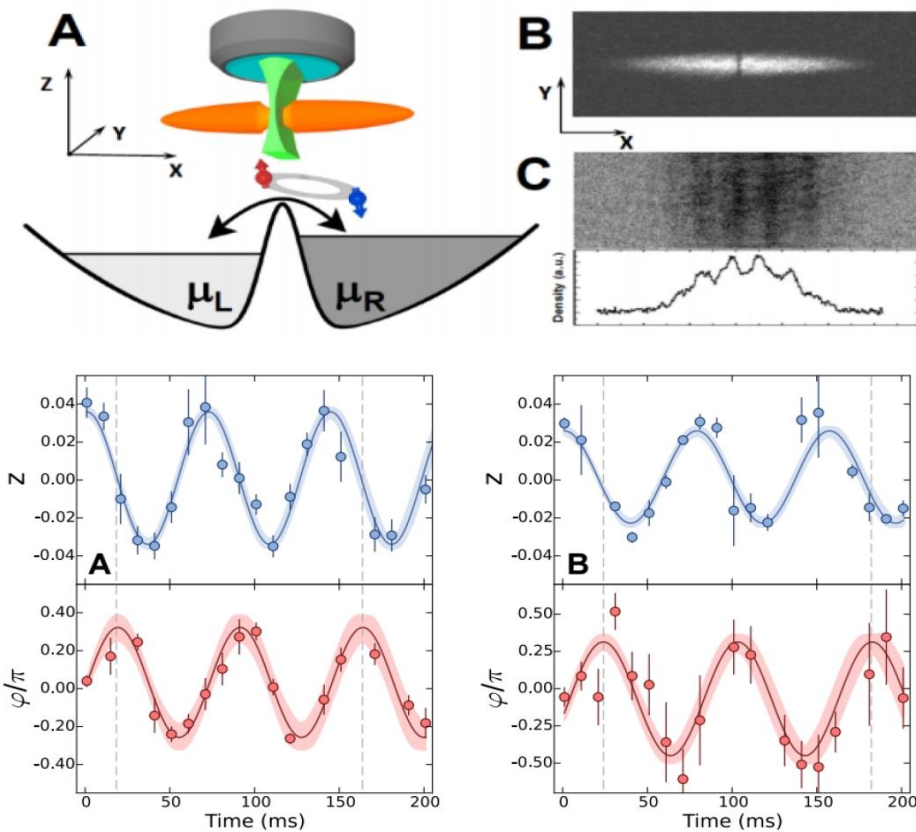
(Received 1 December 1995)

Optical model and exact finite range distorted-wave Born approximation analyses were performed on neutron pair exchange between identical cores for ^{32}S and ^{34}S nuclei and on proton pair exchange between identical cores for ^{30}Si and ^{32}S . The extracted spectroscopic factors were compared with theoretical ones deduced from Hartree-Fock calculations on these pairs of nuclei. The enhancement of the experimental cross sections with respect to the theoretical ones strongly suggests evidence for a nuclear Josephson effect.

Ultracold atomic gases: two regimes for realization of the Josephson junction

Weak coupling (weak link)

Strong coupling



Observation of **AC Josephson effect** between two 6Li atomic clouds.

It need not to be accompanied by creation of a topological excitation.

G. Valtolina et al., Science 350, 1505 (2015).

Creation of a „heavy soliton“ after merging two superfluid atomic clouds.

T. Yefsah et al., Nature 499, 426 (2013).

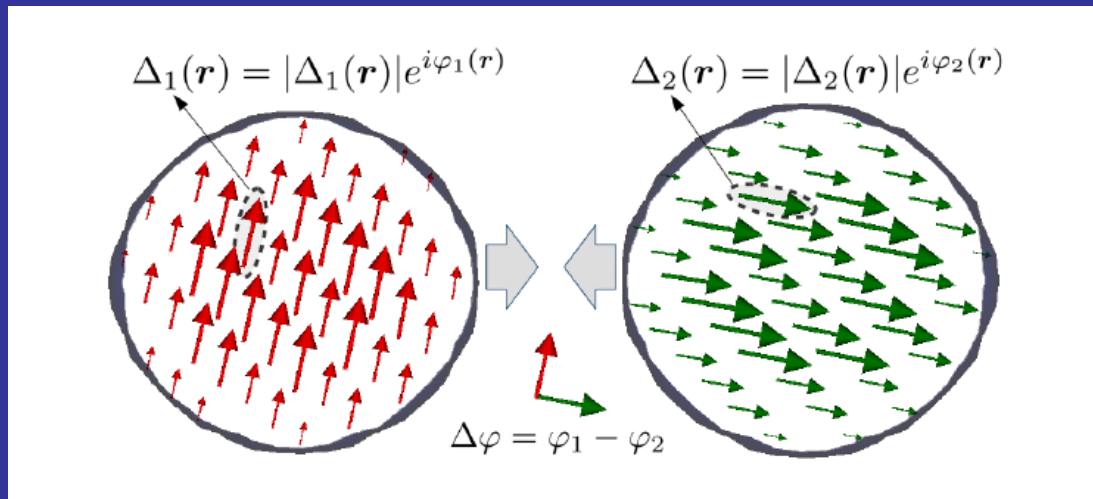
Usually, nuclear applications are limited to the first regime (weak link) and focused on the detection of the Josephson current in the form of enhanced cross section for pair transfer.

We are, however, interested in the **second regime** and nuclear collisions **ABOVE** the barrier.

Consequently the main questions are:

- how a possible solitonic structure can be manifested in nuclear system?
- what observable effect it may have on heavy ion reaction:
kinetic energy distribution of fragments, capture cross section, etc.?

Clearly, we cannot control phases of the pairing field in nuclear experiments and the possible signal need to be extracted after averaging over the phase difference.

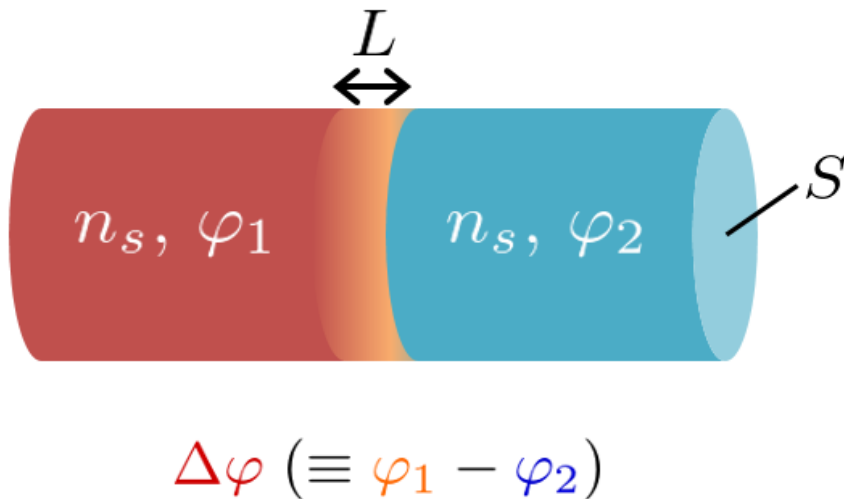


Estimates for the magnitude of the effect

At first one may think that the magnitude of the effect is determined by the nuclear pairing energy which is of the order of MeV's in atomic nuclei (according to the expression):

$$\frac{1}{2} g(\varepsilon_F) |\Delta|^2; \quad g(\varepsilon_F) - \text{density of states}$$

On the other hand the energy stored in the junction can be estimated from Ginzburg-Landau (G-L) approach:

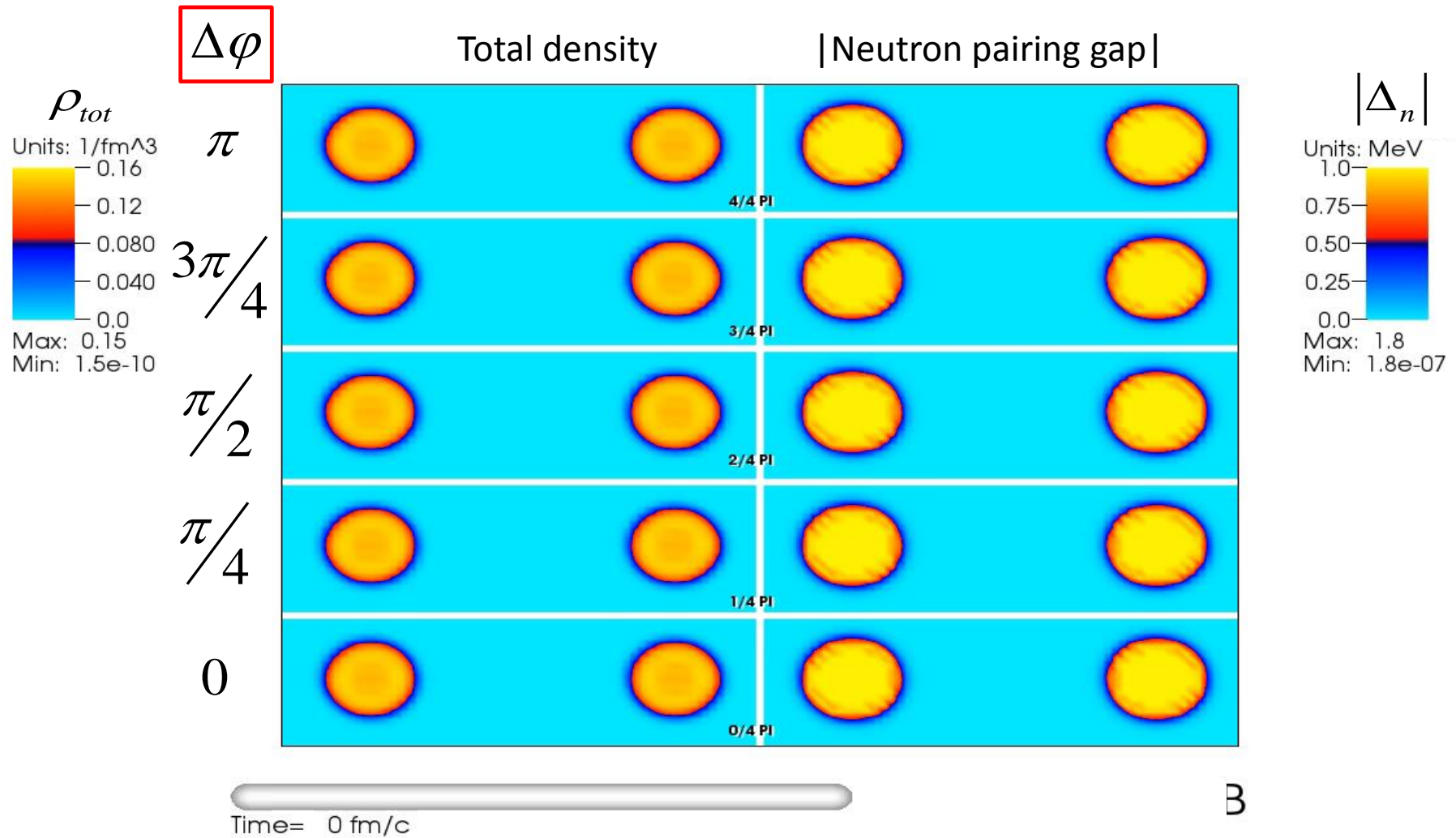


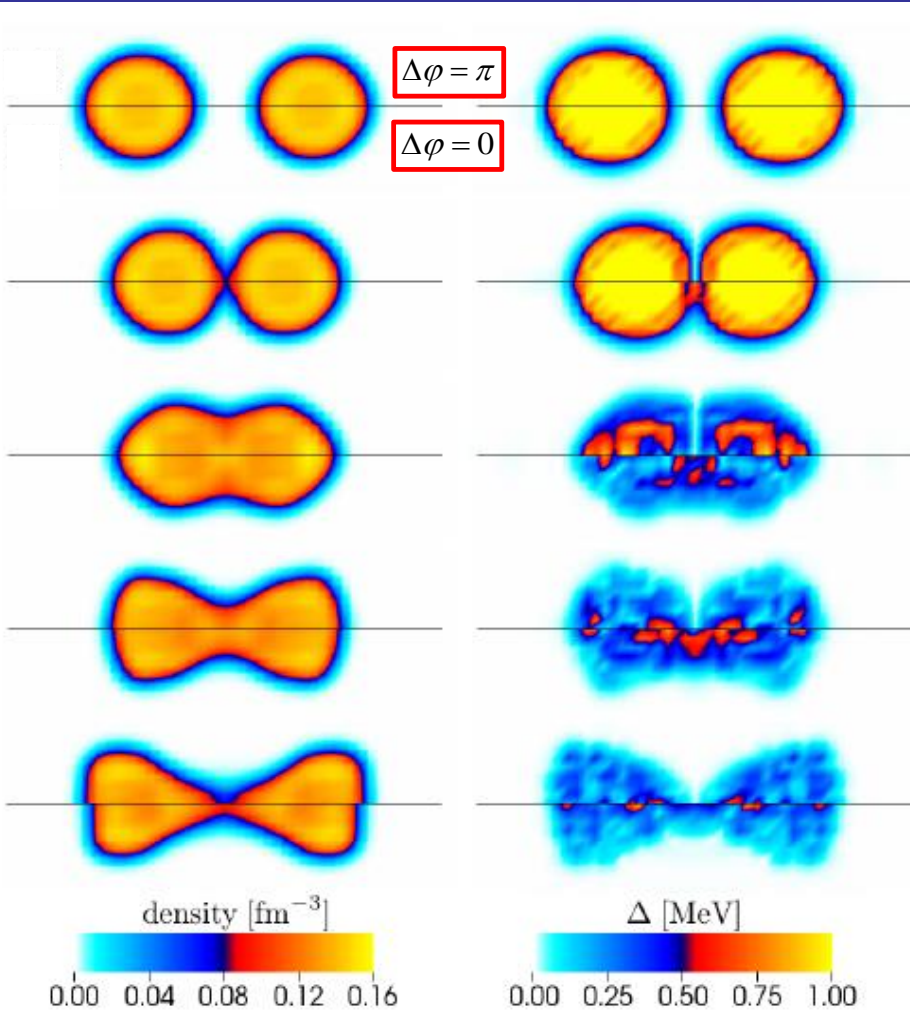
$$E_j = \frac{S \hbar^2}{L 2m} n_s \sin^2 \frac{\Delta\varphi}{2}$$

For typical values characteristic for two heavy nuclei:

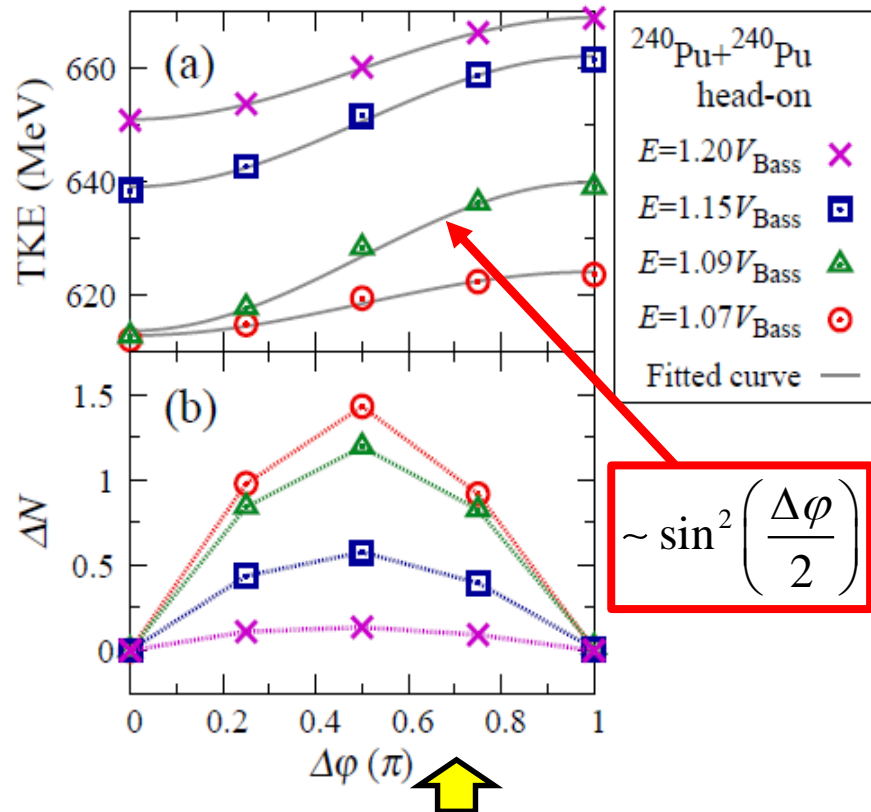
$$E_j \approx 30 \text{ MeV}$$

$^{240}\text{Pu} + ^{240}\text{Pu}$ at energy $E \approx 1.1V_{\text{Bass}}$





Total kinetic energy of the fragments (TKE)



Average particle transfer between fragments.

Creation of the solitonic structure between colliding nuclei prevents energy transfer to internal degrees of freedom and consequently enhances the kinetic energy of outgoing fragments.

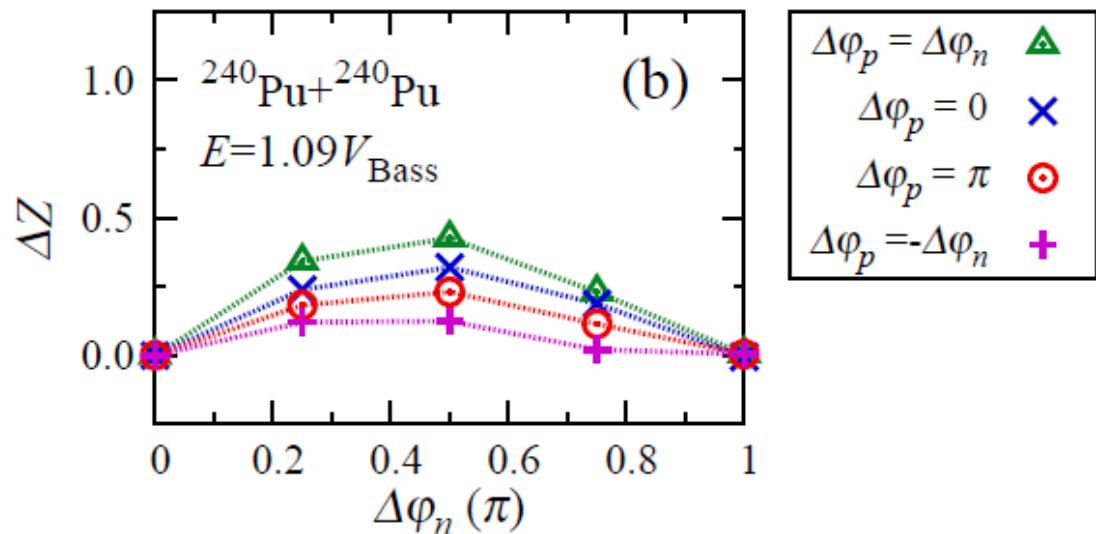
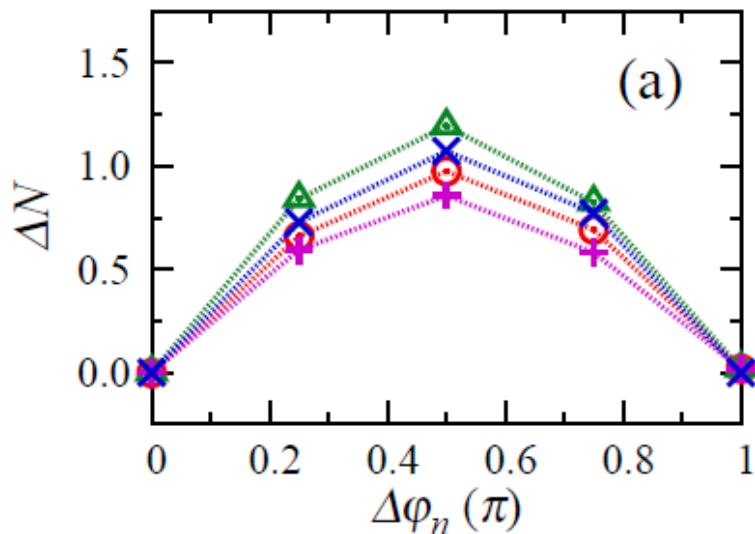
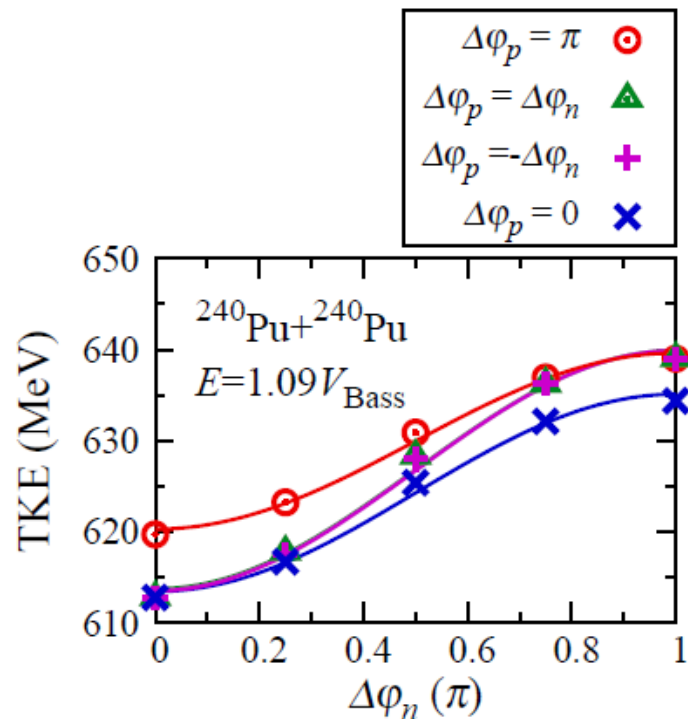
Surprisingly, the gauge angle dependence from the G-L approach is perfectly well reproduced in the kinetic energies of outgoing fragments!

Proton pairing gap contribution to TKE

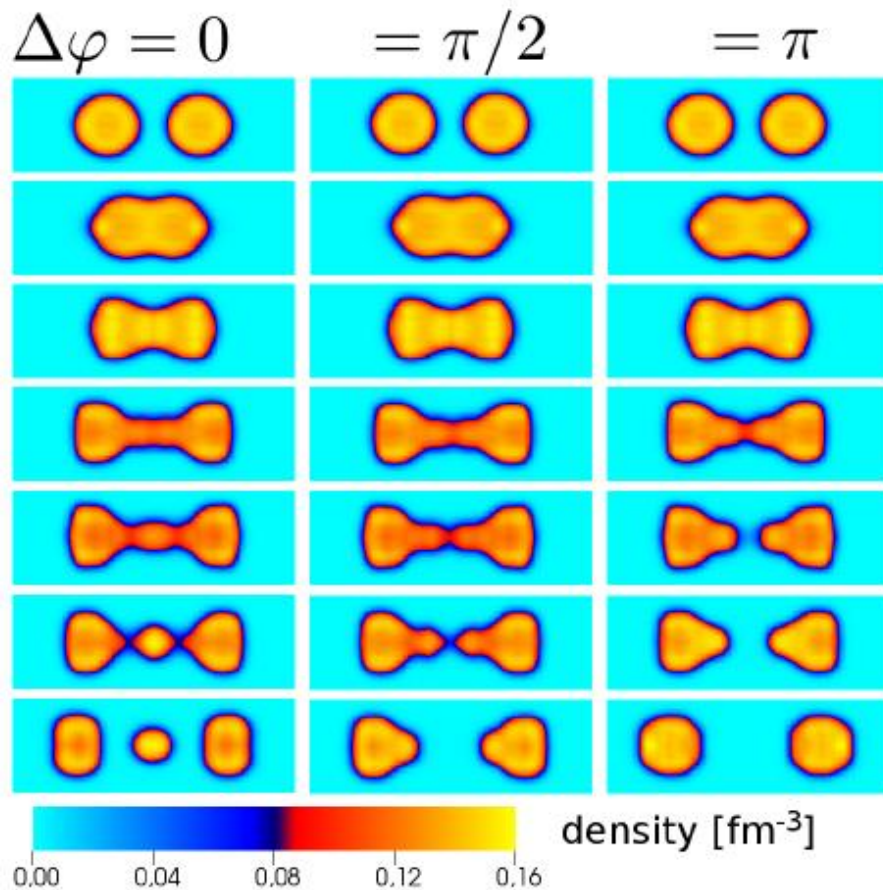
The effect is predominantly due to neutron pairing.

Neutron transfer

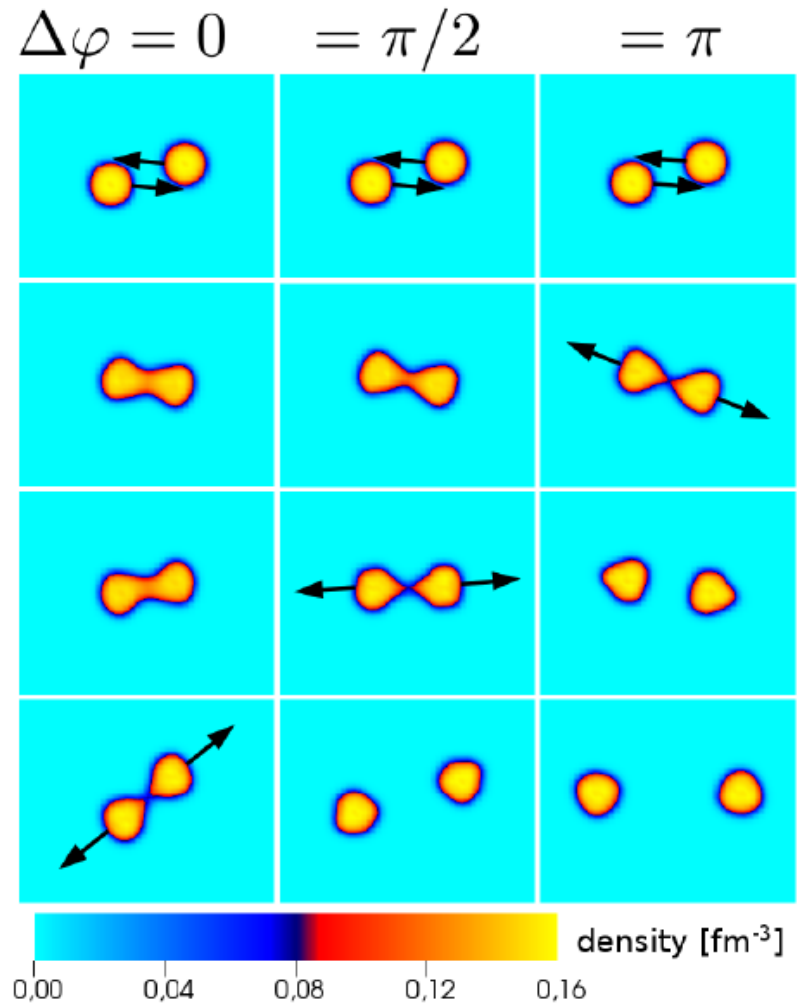
Proton transfer



Noncentral collisions



At higher energies (1.3-1.5 of the barrier height) the phase difference modifies the reaction outcomes suppressing the reaction channel leading to 3 fragments.



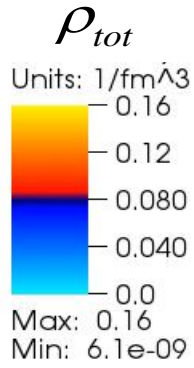
For noncentral collisions the trajectories of outgoing nuclei are affected due to the shorter contact time for larger phase differences.

$^{90}\text{Zr} + ^{90}\text{Zr}$ at energy $E \approx V_{\text{Bass}}$

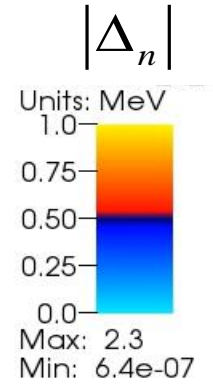
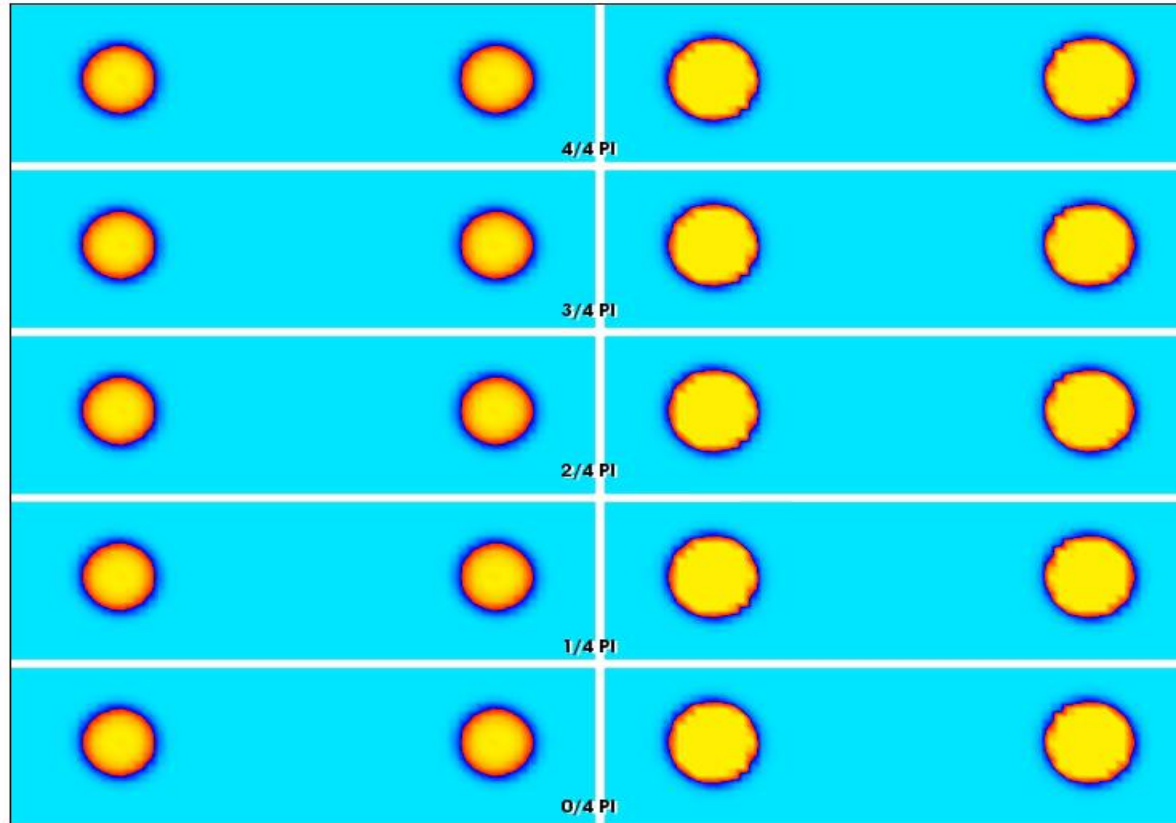
$\Delta\varphi$

Total density

|Neutron pairing gap|



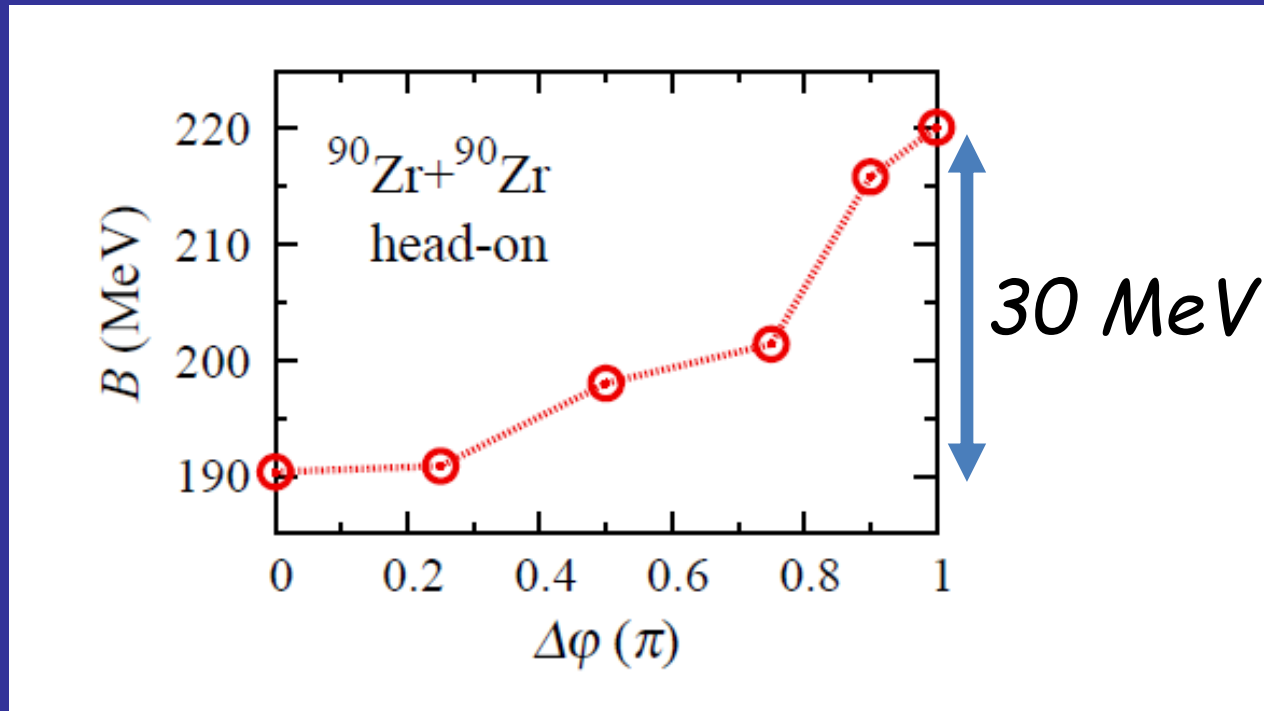
π
 $3\pi/4$
 $\pi/2$
 $\pi/4$
0



Time= 0 fm/c

Modification of the capture cross section!

Effective barrier height for fusion as a function of the phase difference



What is an average extra energy needed for the capture?

$$E_{extra} = \frac{1}{\pi} \int_0^{\pi} (B(\Delta\phi) - V_{Bass}) d(\Delta\phi) \approx 10 \text{ MeV}$$

How the angle dependence affects the shape of the excitation function?

$$\frac{d}{dE} (E\sigma(E)) \propto \Delta\varphi_{tr} + \dots$$

Summarizing

Pairing field dynamics play an important role in nuclear dynamics including both induced fission (see Aurel's talk) and collisions.

Clearly the aforementioned effects **CANNOT** be grasped by any version of simplified (and commonly used) TDHF+BCS approach.

The phase difference of the pairing fields of colliding medium or heavy nuclei produces a similar solitonic structure as the system of two merging atomic clouds.

The energy stored in the created junction is subsequently released giving rise to an increased kinetic energy of the fragments and modifying their trajectories. The effect is found to be of the order of 30MeV for heavy nuclei and occur for energies up to 20-30% of the barrier height.

Consequently the effective barrier for the capture of medium nuclei is enhanced by about 10MeV.

Josephson current is weak and DOES NOT contribute noticeably to collision dynamics (consistent with other studies).

Open questions

Time dependent DFT describes nuclear collision in the broken symmetry framework.

What is the effect of the particle nonconservation ?

Whether the broken symmetry framework provides a reasonable description depends on the time scale associated with the related Goldstone mode.

Namely, in the case of collision of well deformed nuclei it is sufficient to average results over various mutual orientations, as the time scale of the related Goldstone mode is many orders of magnitude longer than the collision time.

Here, the time scale is related to the inverse of the neutron separation energy. However, since both pairing fields rotate in gauge space it is rather the difference of the separation energy which matters (this can be made arbitrarily long in the case of symmetric collisions)

On the other hand:

Aurel's argument (see Aurel's talk) based on the concept of „phase locking“ suggest that the projection on the particle number difference between colliding nuclei need to be considered.

Effective mass of a nucleus in superfluid neutron environment

Suppose we would like to evaluate an effective mass of a heavy particle immersed in a Fermi bath.

It means we would like to replace the original problem with the simplified equation:

$$i\hbar \frac{\partial}{\partial t} \Psi = \hat{H} \Psi \quad \xrightarrow{?} \quad M \frac{d^2 q}{dt^2} - F_D \left(\frac{dq}{dt}, \dots \right) + \frac{dE}{dq} = 0$$

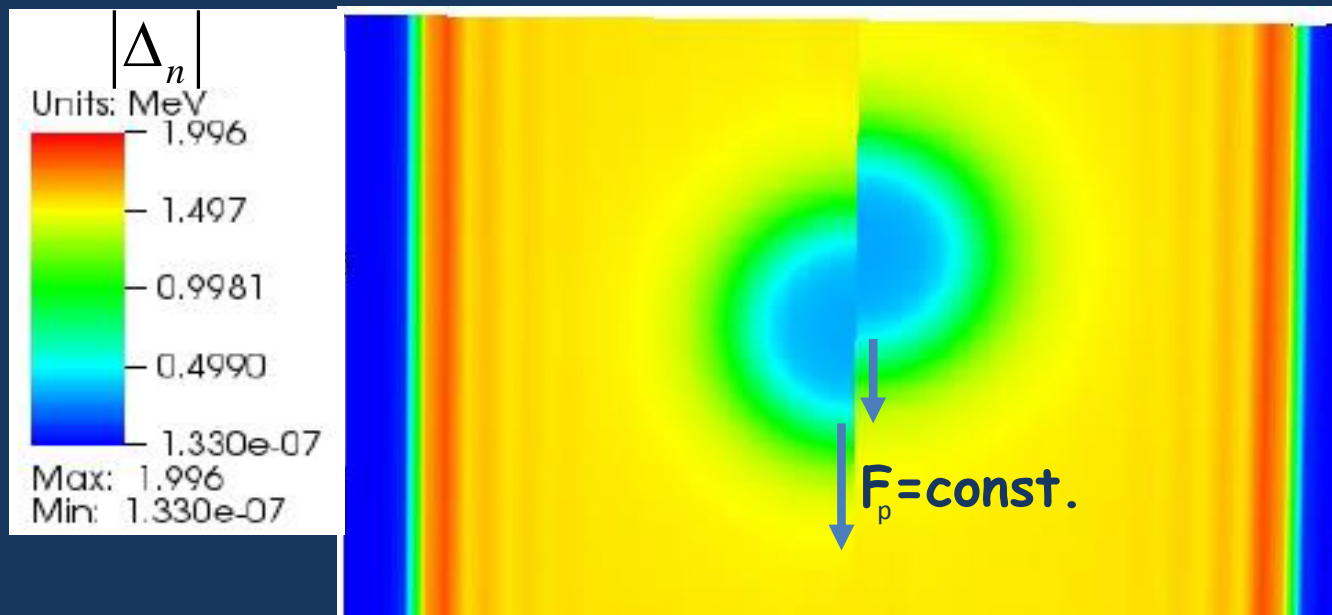
In general it is a complicated task as the first (mass term) and the second term (dissipation) may not be unambiguously separated.

However, for the superfluid system it can be done as for sufficiently slow motion (below the critical velocity) the second term may be neglected due to the presence of the pairing gap.

Another difficulty:

In the context of the neutron star crust it is also not known a priori what is the effective size of the moving impurity, ie. how many neutrons will be dragged.

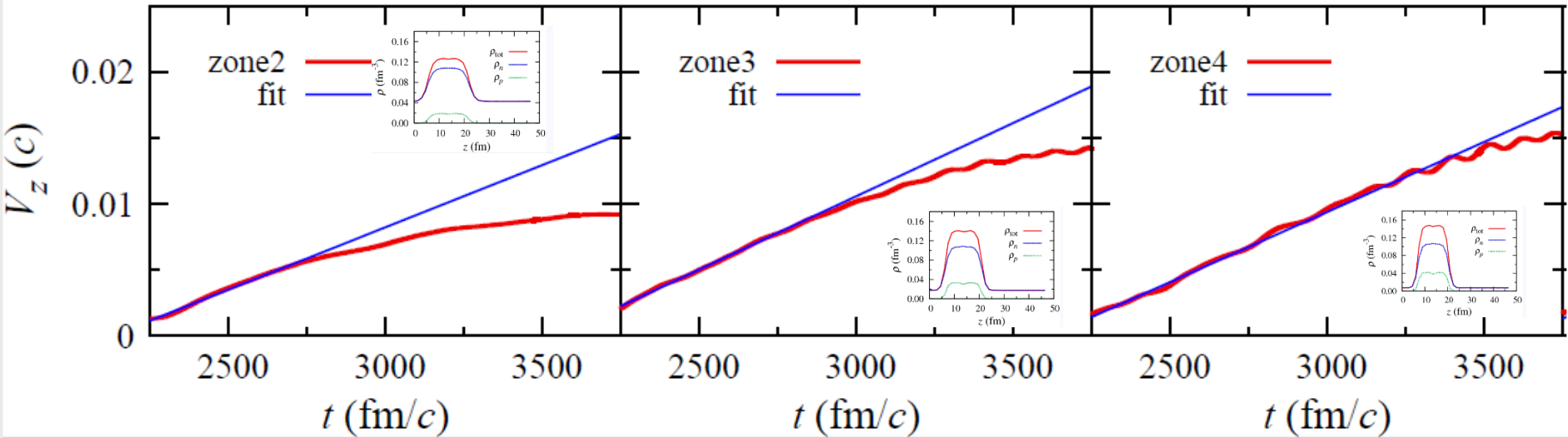
Determination of nuclear effective mass in the superfluid neutron environment from time dependent DFT:



$$M_{eff} = \frac{F_p}{\left(\frac{dV_{CM \text{ protons}}}{dt} \right)}$$

Exerting a constant force on protons we measure the velocity of the proton CM as a function of time and determine the mass.

Velocity of protons for various zones in neutron star crust ($F = 2 \text{ MeV/fm}$)



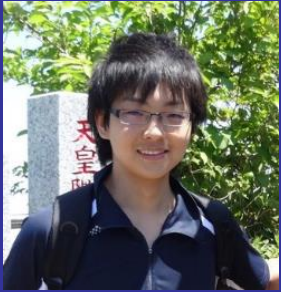
Advantages:

- Size of impurity is selfconsistently determined.
- No need to specify boundary conditions between impurity and superfluid environment.
- No need to divide the system into bound and unbound neutrons.
- No ambiguities concerning relation between superfluid density (which enters hydrodyn. description) and neutron and proton densities.
- Adding other obstacles/impurities is straightforward.
- The critical velocity at which dissipative effects set in can be extracted.
- Various collective degrees of freedom involving impurity itself (eg. deformation) and its coupling to the environment are selfconsistently included.
- This approach offers an easy way to determine important collective modes, which may be excited by moving impurity (for example: we have detected low lying isovector GDR at energies of about 1 MeV).

Zone	Element	Z	N	R_{WS} [fm]	ρ_b [$\text{g} \cdot \text{cm}^{-3}$]	$k_{F,n}$ [fm^{-1}]
11	^{180}Zr	40	140	53.6	$4.67 \cdot 10^{11}$	0.12
10	^{200}Zr	40	160	49.2	$6.69 \cdot 10^{11}$	0.15
9	^{250}Zr	40	210	46.4	$1.00 \cdot 10^{12}$	0.19
8	^{320}Zr	40	280	44.4	$1.47 \cdot 10^{12}$	0.23
7	^{500}Zr	40	460	42.2	$2.66 \cdot 10^{12}$	0.31
6	^{950}Sn	50	900	39.3	$6.24 \cdot 10^{12}$	0.43
5	^{1100}Sn	50	1050	35.7	$9.65 \cdot 10^{12}$	0.51
4	^{1350}Sn	50	1300	33.0	$1.49 \cdot 10^{13}$	0.60
3	^{1800}Sn	50	1750	27.6	$3.41 \cdot 10^{13}$	0.80
2	^{1500}Zr	40	1460	19.6	$7.94 \cdot 10^{13}$	1.08
1	^{982}Ge	32	950	14.4	$1.32 \cdot 10^{14}$	1.33

Pastore, Baroni, Losa, arXiv:1108.3123

Collaborators:



Kazuyuki Sekizawa
(WUT)



Gabriel Wlazłowski
(WUT)



Aurel Bulgac
(U. Washington)



Kenneth J. Roche
(PNNL)



Ionel Stetcu
(LANL)